Journal of the Korea Academia-Industrial cooperation Society
Vol. 22, No. 3 pp. 770-776, 2021

https://doi.org/10.5762/KAIS.2021.22.3.770
ISSN 1975-4701 / eISSN 2288-4688

Analysis of the characteristics of inertial sensors to detect position changes in a large space

Jong-Kyun Hong
Division of Physics, Hanyang University

넓은 공간에서 위치 변화를 감지하기위한 관성 센서의 특성 분석

홍종균
한양대학교 물리학과

Abstract Positioning systems have been actively researched and developed over the past few years and have been used in many applications. This paper presents a method to determine a location in a large space using a sensor system consisting of an accelerometer and a single-axis gyroscope. In particular, to consider usability, a sensor device was loosely worn on the waist so that the experimental data could be used in practical applications. Based on the experimental results of circular tracks with radiuses of 1m and 3m, in this paper, an algorithm using the threshold of rotation angle was proposed and applied to the experimental results. A tracking experiment was performed on the grid-pattern track model. For raw sensor data, the average deviation between the final tracking point and the target point was approximately 15.2 m, which could be reduced to approximately 4.0 m using an algorithm applying the rotation angle threshold.

요 약 위치 파악을 위한 시스템은 지난 몇 년 동안 적극적으로 연구 및 개발되었으며 많은 응용 분야에 적용되고 있다. 본 논문은 가속도계와 단일 축 자이로 스코프로 구성된 센서 시스템을 사용하여 실내와 실외의 넓은 공간에서 위치를 파악하는 방법을 제안한다. 가속도계와 자이로 스코프를 사용하여 사람의 움직임을 인식하는 시스템을 설계 한 후 기하학적 알고리즘을 센서 데이터에 적용하여 오차율을 줄이고자 하였다. 특히 활용성을 고려하기 위하여 센서 기기를 허리에 느슨하게 착용함으로써 실험 데이터가 실제 응용 분야에 유용하게 사용될 수 있도록 고려하였다. 반지름이 1m, 3m인 원형 트랙의 실험 결과를 바탕으로 본 논문에서는 회전 각도의 임계 값을 이용한 알고리즘을 제안하고 실험 결과에 적용하였다. 그리드 패턴 트랙 모델에 대한 추적 실험을 수행했으며, 최종 추적 지점과 목표 지점의 평균 편차는 원시 센서 데이터의 경우 약 15.2m로 확인 되었으며, 회전 각도 임계 값을 사용하는 알고리즘을 사용하여 약 4.0m로 줄일 수 있었다.

Keywords : Positioning Systems, Inertial Sensors, Accelerometer, Gyroscope, Movement Tracking, Probability-Based Algorithms

1. Introduction

Positioning systems have been actively researched and developed over the past few years and there are many possible applications [1,2]. Specifically, localization systems may be used for quickly

본 논문은 2020 학년도 제주대학교 삼정 학술연구비 지원사업에 의하여 연구되었음.
*Corresponding Author : Kyung-Soo Hwang(Jeju National Univ.)
email: kshwang@jejunu.ac.kr
Received November 25, 2020 Revised December 23, 2020
Accepted March 5, 2021 Published March 31, 2021

rescuing urgent patients after emergency calls [3]. It is also possible to offer users customized services while shopping and in public spaces, as well as useful information in unfamiliar or complex areas such as airports and train stations [4]. Among the various types of localization systems, wireless communication systems providing absolute location values are the main focus of current research. Localization methods using wireless communication systems, including received signal strength (RSS)-based localization methods and receiving time-based methods such as time of arrival (TOA) and time difference of arrival (TDOA), have been considered [1].

RSS-based localization methods usually use databases that store RSS values for each surveyed position. Due to the movements of people and objects, RSS values may fluctuate, and dilution of precision (DOP) values may be increased [5]. Time-based localization systems calculate the distance between a transmitter-receiver pair using the difference between the transmit time of the transmitter and the receive time of the receiver. Furniture and fixtures in indoor spaces may obstruct the line-of-sight (LOS) between a receiver-transmitter pair. This non-LOS problem may cause considerably large error ranges to become even wider [6]. In order to solve such problems, we propose a localization system using a wearable sensor board which supplies location values at periodical time intervals.

In the case of these communication system-based localization methods, errors in location data become large in environments where wireless communication is not smooth. Therefore, it is expected that a sensor-based positioning system that is not involved in the wireless communication environment can prevent the loss of location data. Also, even when the wireless communication environment is good, the displacement data obtained from the sensor-based positioning system will help to improve the error of the position data. Sensors are widely applied for various purposes [7-9]. For example, sensor systems are installed in the suspensions of vehicles and aircraft for action stabilization and in game system motion controllers in order to recognize human behavior. The motion of machines as well as the movement patterns of humans can be analyzed and recognized by installing an appropriate sensor system. While many groups are working on the recognition of only specific human movement patterns (i.e., running, walking, sitting, bending) using sensor systems, there has been little research into sensor system-aided localization systems.

We suggest that sensor systems and localization algorithms need to calibrate location error values from the localization systems as well as offer real-time location-based services. We propose a sensor system that is composed of one triple axis accelerometer and one single axis gyroscope mounted on a wearable sensor board in order to supply relative location values. Two algorithms are proposed in order to cover wide space environments such as halls and lobbies. We also discuss possibilities for applying the suggested sensor system to localization systems in wide spaces as well as in recognizing human movement patterns.

The paper is organized as follows. First, the sensor system and sensor data processing methods are introduced, and then the characteristics of the sensors are analyzed and calibrated through unit experiments. Next, a localization method using the suggested algorithms with special consideration of wide spaces is discussed. Finally, the paper concludes with a brief discussion.

2. Point

2.1 Sensor System and Data Process

The microcontroller unit (MCU) used is a

LM8962 processor made by Luminary Micro, which uses a 32-bit Cortex-M3 profile. We also use a myAccel3LV02 accelerometer with a 3-axis sensing device. The accelerometer has an option for acceleration measurement ranges of ±2g and ±6g, where g is the acceleration of gravity in m/sec^2. We set the range to ±2g for this research. The accelerometer communicates with the MCU through the I2C serial communication interface. The gyroscope used is a myGyro300SPI, with a maximum detectable angular velocity of ±300 degree/sec. The gyroscope sensor was connected to the MCU using an SPI serial communication interface.

It is expected that the waist of human body will accurately express both the movement status and turning angle of the entire body, and so the sensor board was placed firmly on a waist belt to give better experimental results. However, in practical contexts, arbitrary degrees of sway are anticipated. When the sensor board is worn on the waist, the x-axis of the accelerometer is set as the axis that is maximally affected by the acceleration of gravity, the y-axis is set to sense forward and backward movement, and the z-axis is set to sense right and left movement. The axis of rotation for the gyroscope is the same as the x-axis of the accelerometer, so the gyroscope is mounted on the sensor board in order to recognize turning directions (right or left), as well as to measure the turning angle. However, because the sensor board sways, the axes of the sensors also sway according to the movement of the body. Therefore, unwanted noise might be included in the sensor output data. Compensating for this weakness is a challenge of this research.

Current location information can be obtained by converting the sensor data into relative moving distances and changing angles. We use i to index the output data of the sensors, and the output data from the accelerometer (d_{i-a}) is the proportional constant that explains the relative value for the acceleration of gravity (g = 9.8 m/s^2). So, the acceleration value of the sensor can be calculated by multiplying d_{i-a} and g. Also, the acceleration value multiplied by the sensor data collection interval (Δt) equals the current velocity value. Moreover, the relative moving distance (D) for a variable measurement period can be found using the sum of all the velocity values obtained at the interval Δt within the measurement period. We name the variable measurement period as *1-period*, and so can express the relative moving distance as

$$D = \sum_{i}^{1-period} (d_{i-a} g \Delta t) \; [m] \tag{1}$$

To gather enough data to classify human movements, *1-period* was set to 0.5 second. The sensor data collection interval was set to 10 ms, and so the current velocity value can be calculated at 10 ms intervals. The present location can be calculated via Eq. (2) with the relative moving distance calculated using Eq. (1).

$$\begin{aligned} x_{CP} &= x_{PP} + D\cos\theta_{PD} \; [m] \\ y_{CP} &= y_{PP} + D\sin\theta_{PD} \; [m] \end{aligned} \tag{2}$$

where x_{PP} and x_{CP} are the x-axis values of the previous and present locations, respectively, and y_{PP} and y_{CP} are the y-axis values. θ_{PD} represents the previous direction of movement, and in the case of straight movement, this direction is fixed as the initial direction.

Like experiments for straight movement, the experiments examining curvilinear movements along a round pre-defined track confirm the differences between the output data of the gyroscope and the actual turning angle values. Experiments examining curvilinear movements with right or left turns along the round track were performed repeatedly. The relative turning angle (A) can be calculated using Eq. (3) with the output data of the gyroscope.

$$A = \sum_{i}^{1-period} (d_{i-g} \Delta A \Delta t) \ [\mathrm{degree}] \qquad (3)$$

where $d_{i\text{-}g}$ is the output data of the gyroscope, and ΔA is the resolution of the angular velocity of the gyroscope (0.2439 degree/sec). The present location can be calculated using Eq. (4) with the relative turning angle calculated using Eq. (3).

$$x_{CP} = x_{PP} + 2\left(\frac{D}{A}\right) \cdot \sin\left(\frac{A}{2}\right) \cdot \cos\left[\theta_{PD} + \left(90 - \frac{180 - A}{2}\right)\right] \ [m] \qquad (4)$$

$$y_{CP} = y_{PP} + 2\left(\frac{D}{A}\right) \cdot \sin\left(\frac{A}{2}\right) \cdot \sin\left[\theta_{PD} + \left(90 - \frac{180 - A}{2}\right)\right] \ [m]$$

2.2 Basic Sensor Characteristics

This section describes the experimental methods and their results for curvilinear movements detected using the accelerometer and the gyroscope. The data collection interval was set to 0.5 second to collect enough data to recognize human motion patterns. The radii and change of direction angles in wide spaces have a large number of degrees of freedom. So, basic experiments to recognize covered distances and changed angles on circular tracks were conducted. In consideration of the resolution limit for localization in wide spaces, the radii of the circles were set to 1 m and 3 m. Also, the movement paths are from the start point to points at turning angles of 90°, 180°, 270°, and 360° along the circular track.

To recognize turning angles and changes of direction, the velocities and distances of the subjects' movements are first calculated using the output data from the accelerometer and the gyroscope. Movement pattern recognition (walking vs. running) is solved using the accelerometer. Next, the radii of the curvilinear movements are defined, and the turning angles are calculated.

The radii of the curvilinear movements are obtained using the histogram shown in Fig. 1. The histogram shows the repetition numbers for values of each angle change for each *1-period* (i.e., every 0.5 seconds). For example, at a radius of 3m, the repetition number for an angle change of 2° is 10. From the histogram, the threshold value to calculate the turning angles is 16°. In other words, if the angle change value over 1-period is smaller than 16°, then the radius is defined as 3 m, and if the value is larger than 16°, then the radius is defined as 1 m. Finally, using the movement distance and the turning radius calculated based on collected data over *1-period*, the turning angle is calculated as the movement distance divided by the turning radius.

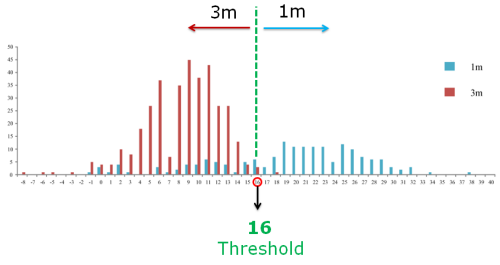

Fig. 1. Histogram along the variation angle for radii of 1 m and 3 m.

The algorithm was used in experiments along the circular tracks. Fig. 2 shows the experimental results using only the raw data of the sensors, while Fig. 3 shows the results of our algorithm. All the results in Fig. 2 and Fig. 3 are for an angle variation of 360°.

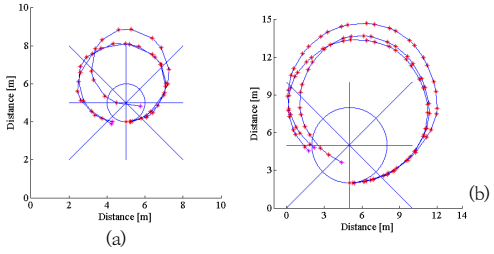

Fig. 2. Tracking results using only the raw data of the sensors. (a) Circular track with radius of 1 m. (b) Circular track with radius of 3 m.

As seen in Fig. 2, the inertial sensors cannot properly recognize human movements. In particular, the sway of the accelerometer gives greater moving distances than the truth. Also, the gyroscope cannot exactly express the turning angles of humans. As a result, all the tracking results deviate considerably from the real circular tracks.

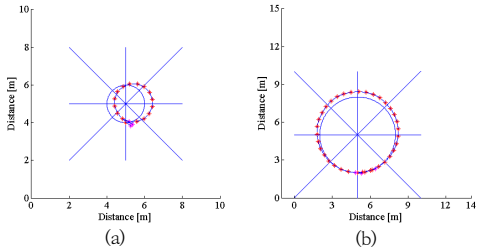

Fig. 3. Tracking results using the TAT algorithm. (a) Circular track with radius of 1 m. (b) Circular track with radius of 3 m.

Fig. 3 shows the results of using the turning angle threshold (TAT) algorithm proposed in this paper. It is easily confirmed that these results closely match the true circular tracks. However, because some of calculated data are not included in a proper range referred to the threshold value which is decided from Fig. 1, there is a small amount of error.

2.3 Tracking Experiments

In this section, we discuss experimental results considering wide spaces. Data was obtained from both the accelerometer and the gyroscope during tracking along the set routes, and the distances and angles were calculated using the equations described in the previous section. Grid patterned track models have been set for tracking experiments of movement paths in wide spaces. Also, to consider the resolutions for tracking movement paths of 1 m and 3 m, the sizes of the squares which are elements of two types of the grid patterned track models are defined as 1 m × 1 m and 3 m × 3 m. The shapes of the two types of grid patterned track models and the movement paths are shown in the insets of Fig. 4.

Fig. 4 shows the results of tracking experiments of the movement paths on the grid patterned track models. Fig. 4 (a) is for a 1 m × 1 m square, while Fig. 4 (b) is for a 3 m × 3 m square. Also, both the x-axis and y-axis are given in meters. It is clearly seen that the results from just the raw data deviate seriously from the true paths. As discussed in the previous section, such results are caused by the swaying of the sensor board, which means the accelerometer and the gyroscope cannot correctly recognize human movements.

The results after application of the TAT algorithm are shown in Fig. 4. Because there are some data outside of the proper area referring to the threshold value of the TAT algorithm, the resultant tracking paths do not track the actual movement paths exactly. However, the results are much better, and the TAT algorithm is especially good at recognizing changing directions.

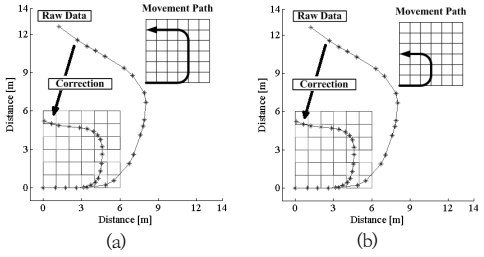

Fig. 4. Results of the tracking experiments in wide spaces, both with and without the TAT algorithm. (a) Grid pattern tracking for the 1 m × 1 m square. (b) Grid pattern tracking for the 3 m × 3 m square.

Table 1. Distance deviations of the final tracking points from the destination points.

Square Size	1 m			3 m		
Case	1	2	3	1	2	3
Raw Data [m]	10.42	12.05	9.83	19.68	19.60	19.68
TAT Applied [m]	5.6	2.25	4.9	5.6	0.54	5.13

The tracking experiments were performed three times for each track. Table 1 shows the distance deviations of the final tracking points from the destination points of the pre-defined movement paths. For just the raw data, the average distance deviations were approximately 10.76 m and 19.65 m for the squares of sizes 1 m × 1 m and 3 m × 3 m, respectively. On the other hand, with the TAT algorithm, the average distance deviations were approximately 4.25 m and 3.75 m for the squares of sizes 1 m × 1 m and 3 m × 3 m, respectively. Thus, it is confirmed that the distance deviation is considerably reduced by using the TAT algorithm.

Table 2 shows the results for the calculated distances and the distance errors per unit distance of total movement along the pre-defined courses. The distances of the pre-defined courses were 12.14 m and 24.42 m for the 1m × 1m and 3m × 3m squares, respectively. From the results in Table 2, the average values of the resultant movement distances were 16.08 m and 26.97 m, and the average distance errors per unit distance were 0.32 m and 0.1 m, respectively.

Table 2. The calculated distances and the distance errors per unit distance of total movement.

Square Size	1 m			3 m		
Case	1	2	3	1	2	3
Movement Distance [m]	16.65	15.13	16.46	26.19	26.06	28.66
Distance Error [m]	0.37	0.24	0.35	0.07	0.06	0.17

3. Conclusion

This paper presents a localization method for wide spaces using a sensor system consisting of an accelerometer and a single axis gyroscope. We designed a system to recognize human movements using the accelerometer and gyroscope and then applied sensor data to the suggested geometric algorithm. We determined subject locations by calculating both velocity and direction. The sensor board, consisting of an accelerometer and gyroscope, was worn loosely at the waist, which makes the system useful for practical applications. Basic experiments to recognize movement on circular tracks with radii of 1 m and 3 m were conducted. The results confirmed that the tracking results using the suggested turning angle threshold (TAT) algorithm closely match the circular tracks. In grid patterned track experiments,, the average distance deviations with only the raw data were approximately 10.76 m and 19.65 m for grids of sizes 1 m × 1 m and 3 m × 3 m, respectively. On the other hand, after applying the TAT algorithm, the average distance deviations were approximately 4.25 m and 3.75 m, respectively. Thus, it is confirmed that the distance deviation is considerably reduced by using the TAT algorithm.

The possibility of localization using only sensors worn on the body was validated via independent experiments. Our methodology will provide more precise location detection when used along with GPS and wireless communications, both outdoors and indoors. The suggested localization method can be used in various applications, such as indoor/outdoor positioning systems, military applications, fire-fighting technologies, and healthcare.

References

[1] J. Xiao, Z. Liu, Y. Yang, D. Liu, X. Han, "Comparison and analysis of indoor wireless positioning techniques", *International Conference on Computer Science and Service System*, IEEE, Nanjing, China, pp. 293-296, June 2011.
DOI: https://doi.org/10.1109/CSSS.2011.5972088

[2] R. Mautz, "Overview of current indoor positioning systems", *Geodesy and Cartography*, Vol. 35, No. 1, pp 18-22, March 2009.
DOI: https://doi.org/10.3846/1392-1541.2009.35.18-22

[3] L. Coyle, S. Neely, P. Nixon, A. Quigley, "Sensor

aggregation and integration in healthcare location based services", *Pervasive Health Conference and Workshops*, IEEE, Innsbruck, Austria, pp. 1-4, Nov. 2006.
DOI: https://doi.org/10.1109/PCTHEALTH.2006.361698

[4] S. Dhar, U. Varshney, "Challenges and business models for mobile location-based services and advertising", *Communications of the ACM*, Vol. 54, No.5, pp.121-128, May 2011.
DOI: https://doi.org/10.1145/1941487.1941515

[5] A. Bose and C. H. Foh, "A practical path loss model for indoor WiFi positioning enhancement," *6th International Conference on Information, Communications & Signal Processing*, IEEE, Singapore, Singapore, pp. 1-5, Dec. 2007.
DOI: https://doi.org/10.1109/ICICS.2007.4449717

[6] H. L. Dehghani, S. Golmohammadi, K. Shadi, "Extract Non-Line-of-Sight state of base stations and error mitigation technique for wireless localization in micro-cell networks," *Computer Communications*, Vol. 35, No. 7, pp. 885-893, Feb. 2012.
DOI: https://doi.org/10.1016/j.comcom.2012.01.021

[7] R. Sekhar, R. K. Musalay, Y. Krishnamurthy and B. Shreenivas, "Inertial sensor based wireless control of a robotic arm," *IEEE International Conference on Emerging Signal Processing Applications*, IEEE, NV, USA, pp. 87-90, Jan. 2012.
DOI: https://doi.org/10.1109/ESPA.2012.6152452

[8] X. Yun, J. Calusdian, E. R. Bachmann, and R. B. McGhee, "Estimation of Human Foot Motion During Normal Walking Using Inertial and Magnetic Sensor Measurements," *IEEE Transactions on Instrumentation and Measurement*, Vol. 61, No. 7, July 2012.
DOI: https://doi.org/10.1109/TIM.2011.2179830

[9] G. To, M. R. Mahfouz, "Design of Wireless Inertial Trackers for Human Joint Motion Analysis," *IEEE Topical Conference on Biomedical Wireless Technologies, Networks, and Sensing Systems*, IEEE, CA, USA, pp. 49-52, Jan. 2012.
DOI: https://doi.org/10.1109/BioWireless.2012.6172737

Jong-Kyun Hong [Regular member]

- Aug. 2002 : Hanyang Univ., Korea, MD
- Feb. 2007 : Hanyang Univ., Korea, PhD
- Mar. 2007 ~ Mar. 2016 : Hanyang Univ., Div. of Elec. and Comp. Eng., Research Associate Professor
- Sep. 2017 ~ current : Hanyang Univ., Dept. of Physics, Research Associate Professor

〈Research Interests〉
Positioning systems, Optical devices, Power Converters